Efficient Wave Modeling using Non-Hydrostatic Pressure Distribution and Free Surface Tracking on Fixed Grids

Hans Bihs*[1], Arun Kamath[1], Ankit Aggarwal[1], and Csaba Pakozdi[2]

[1]Department of Civil and Environmental Engineering, Norwegian University of Science and Technology (NTNU), 7491 Trondheim, Norway
[2]SINTEF Ocean, Trondheim, Norway

Journal of Offshore Mechanics and Arctic Engineering, 2019, **00** , pp. 1-7.
DOI: http://dx.doi.org/10.1115/1.4043179

Abstract

For the estimation of wave loads on offshore structures, relevant extreme wave events need to be identified. In order to achieve this, long term wave simulations of relatively large scales need to be performed. Computational Fluid Dynamics (CFD) based Numerical Wave Tanks (NWT) with an interface capturing two-phase flow approach typically require too large computational resources. In the current paper, a three-dimensional non-hydrostatic wave model is presented which solves the Navier-Stokes equations and employs an interface tracking method based on the continuity of the horizontal velocities along the vertical water column. With this approach, relatively fewer cells are needed in the vicinity of the air-water interface compared to CFD based NWTs. The numerical model solves the governing equations on a rectilinear grid, which allows for the employment of high-order finite differences. The capabilities of the new wave model are presented by comparing the wave propagation in the tank with the CFD approach in a 2D simulation. Further, a 3D simulation is carried out to determine the wave forces on a vertical cylinder. The calculated wave forces using the new approach is compared to that obtained using the CFD approach and experimental data. It is seen that the new approach provides a similar accuracy to that from the CFD approach while providing a large reduction in the time taken for the simulation. The gain is calculated to be about 4.5 for the 2D simulation and about 7.1 for the 3D simulation.

Keywords: 6DOF; floating; level set method; immersed boundary; Computational Fluid Dynamics; REEF3D

*Corresponding author, hans.bihs@ntnu.no
Postprint, published in Journal of Offshore Mechanics and Arctic Engineering, doi:http://dx.doi.org/10.1115/1.4043179

1 Introduction

In the field of wave hydrodynamics and marine free surface flows, the open-source hydrodynamics model REEF3D has been successfully applied for a broad range of flow problems. In Kamath et al. (2015*a*, 2016*b*, 2015*b*), the model was used to analyze non-breaking wave forces on various configurations of multiple vertical circular cylinders. For breaking wave impact on slender cylinders, the numerical model succesfully captured the detailed physics of the overturning waves Kamath et al. (2016*a*); Bihs et al. (2016*b*); Alagan Chella et al. (2017). Further simulation of marine fluid-structure interaction were performed for extreme wave scenarios such as focused waves and wave packets Bihs et al. (2017*a*,*b*). All of the aforementioned studies have in common that they focus on the wave hydrodynamics in the near field of structures. Typically these simulations require relatively fine three-dimensional meshes, especially for correctly capturing and resolving the breaking wave kinematics. When used for these type of cases, REEF3D can be classified as a CFD-based (computational fluid dynamics) numerical wave tank, similar to other models Jacobsen et al. (2012); Higuera et al. (2013).

For a wide range of applications, the detailed resolution of breaking waves is not required. Instead, often a faster solution at a still reasonable accuracy is wanted. To this effect, non-hydrostatic Navier-Stokes equation based solver have been developed. The possibility of using non-hydrostatic shallow equations with multi-layers in the vertical direction has been explored by Zijlema and Stelling Stelling and Zijlema (2003); Zijlema et al. (2005); Zijlema and Stelling (2008) for wave propagation problems in coastal zones. In Ma et al. (2012, 2016), the Navier-Stokes equations are solved in three-dimensions and a tracking function is used for the free surface. The one-phase flow is calculated on a surface- and terrain-following σ-coordinate based grid. As in Zijlema et al. (2005), the mesh has to be dynamically adjusted to the moving free surface. Applications range from wave refraction-diffraction, shoaling to more advanced wave-structure interaction problems. The $\sigma-$coordinate based grid is also presented in other non-hydrostatic models such as Young and Wu (2010) Choi et al. (2011) Ai et al. (2011) and Ai et al. (2014).

In this paper, a free surface tracking algorithm is implemented in REEF3D that uses the divergence of the depth-integrated flow velocities. The resulting equation for the movement of free surface resembles that one found e.g. in Stelling and Zijlema (2003) and Ma et al. (2012). The decisive difference lays in the way the numerical grid is treated. In the current implementation REEF3D::NSEWAVE, the governing free surface equation is solved on a fixed mesh, avoiding remeshing and some of the known inaccuracies of the σ-coordinate grid method, see e.g Stelling and Van Kester (1994) for details.

In order to test the new method, the wave generation and propagation in an empty two-dimensional tank is compared against the free surface location obtained from theory. Wave interaction with a vertical cylinder in a three-dimensional tank is evaluated using the new NSEWAVE approach implemented in the open-source hydrodynamics model REEF3D Bihs et al. (2016*a*); Bihs and Kamath (2017) and compared to the results obtained from the CFD approach and experimental data Chen et al. (2014). The calculated wave forces are compared to experimental data to validate the model.

2 Numerical Model

The model solves the incompressible Reynolds-Averaged Navier-Stokes (RANS) equations to calculate the fluid flow:

$$\frac{\partial u_i}{\partial x_i} = 0 \tag{1}$$

$$\frac{\partial u_i}{\partial t} + u_j \frac{\partial u_i}{\partial x_j} = -\frac{1}{\rho}\frac{\partial p}{\partial x_i} + \frac{\partial}{\partial x_j}\left[(\nu + \nu_t)\left(\frac{\partial u_i}{\partial x_j} + \frac{\partial u_j}{\partial x_i}\right)\right] + g_i \tag{2}$$

where u is the time averaged velocity, ρ is the density of water, p is the pressure, ν is the kinematic viscosity, ν_t is the eddy viscosity, t is time and g is the acceleration due to gravity. Using Chorin's projection method Chorin (1968), the Poisson equation for pressure is obtained. The Poisson pressure equation is solved iteratively with the alogrithms available from the high performance solver library HYPRE Falgout et al. (2010). The PFMG-preconditioned BiCGStab algorithm Ashby and Falgout (1996) is used in this study.

The two-equation k-ω model Wilcox (1994) is used for turbulence modelling. Eddy viscosity limiters proposed by DurbinDurbin (2009), are used to bound the eddy viscosity ν_t to avoid unphysical overproduction of turbulence in the simulation waves which represents a highly strained flow. Additional starin on the flow is introduced from the two-phase modelling approach with a large difference in the density of the two fluids- air and water. To avoid unphysical overproduction of turbulence due to this strain, free surface turbulence damping is carried outusing empirical coefficientsNaot and Rodi (1982).

The discretization of convective terms for the velocity u_i, turbulent kinetic energy k and the specific turbulent dissipation rate ω is carried out by the fifth-order conservative finite difference Weighted Essentially Non-Oscillatory (WENO) schemeJiang and Shu (1996). A TVD third-order Runge-Kutta explicit time schemeHarten (1983) is employed for time advancement of the level set function and the reinitialisation equation. A Cartesian grid is used in the numerical model for spatial discretization. The Immersed Boundary Method (IBM) Peskin (1972) is used to incorporate the boundary conditions for complex geometries. A local directional ghost cell method Berthelsen and Faltinsen (2008) is implemented in the model.

The free surface is obtained using the level set method where the zero level set of a signed distance function, $\phi(\vec{x}, t)$ is used to represent the interface between air and water. Moving away from the interface, the level set function gives the closest distance of the point from the interface. The sign of the function represents the two fluids across the interface. In the interface capturing framework using the level set method to obtain the free surface, the level set function is convected by the external velocity field. The velocity field at the free surface has to be determined accurately for the free surface to be convected and correctly represent the fluid flow. This is achieved by employing a fine mesh around the free surface to resolve the velocities at the free surface to a high degree of accuracy. Using this strategy results in a large number of cells, smaller time steps due to lower CFL numbers required and results in a large computational demand. In order to reduce the computational cost in the RANS framework, the free surface can be evaluated in a different manner. In this approach, the horizontal velocity component is integrated over the entire water column. The flux between each neighbouring column is calculated and then the continuity equation is applied to obtain the free surface.

$$\frac{\partial \zeta}{\partial t} + \frac{\partial}{\partial x}\int_{-d}^{\zeta} u dz + \frac{\partial}{\partial y}\int_{-d}^{\zeta} v dz = 0 \tag{3}$$

Following continuity, a net flux out will result in a drop in the free surface elevation and a net flux in will result in an increase in the free surface elevation. Thus, the free surface is determined taking into account the entire water column and this reduces the stringent requirements on the grid size around the free surface. Due to the reduced requirement of a fine grid around the free surface, simulations can then be run using a much coarser grid with a higher CFL number resulting in larger time steps with similar accuracy in the results.

The strategy used to obtain the free surface described above is similar to the sigma coordinate system used by some large scale ocean and atmospheric models. These models are generally restricted to one phase and require a moving grid to account for the change in the free surface. In the current study, the novelty lies in applying Eq.3 to a two-phase flow scenario on a fixed grid. The level set function is used purely geometrically to distinguish fluid phases on the fixed grid based on the calculated free surface location ζ. The compromise is that the free surface can only be single-valued in the domain. This precludes the resolution of the overturning wave crest of breaking waves.

Wave generation and absorption in the numerical wave tank is carried out using the relaxation method Engsig-Karup (2006) and the relaxation function presented in Jacobsen et al. (2012) shown in Eq.4 below is implemented.

$$\Gamma(x) = 1 - \frac{e^{(1-x)^{3.5}} - 1}{e - 1} \tag{4}$$

where Γ is the relaxation function and x is the distance along the relaxation zone scaled to the total length of the relaxation zone. In the wave generation zone, the relaxation function gradually introduces waves into the numerical wave tank. At the end of the numerical wave tank is the numerical beach, where the waves energy is absorbed gradually to avoid reflected waves in the domain.

3 Results

3.1 Wave propagation in a wave tank without obstacles

In this section, waves are simulated in the numerical wave tank without any structures to ascertain good wave generation and propagation in the wave tank and compare the results with the new approach to the results obtained using the two-phase flow CFD numerical wave tank, where the level set function is convected under the external velocity field. The two-dimensional numerical wave tank used in this study is 18 m long and 1 m high with a water depth $d = 0.505$ m. Regular waves of height $H = 0.07$ m and wavelength $L = 2$ m are generated in the tank using the relaxation method. The simulations are carried out for different grid sizes $dx = dy = dz = 0.1m$, 0.05 m, 0.025 m and 0.0125 m, using the NSEWAVE approach and the CFD approach. The grid sizes are comparable to 5, 10, 20, and 40 layers in a multi-layered non-hydrostatic modelling approach.

Figures 1-4 show the free surface elevation in the numerical wave tank at $x = 5$ m and $x = 9$ for grid sizes $dx = 0.1$ m, $dx = 0.05$m, $dx = 0.025$ m and $dx = 0.0125$ m. The comparison of the free surface elevation in the wave tank at $t = 31.0$ s in the tank, using both NSEWAVE and CFD approach, along with the theoretically expected free surface elevation using the $2nd$-order Stokes wave theory is presented in Fig. 5.

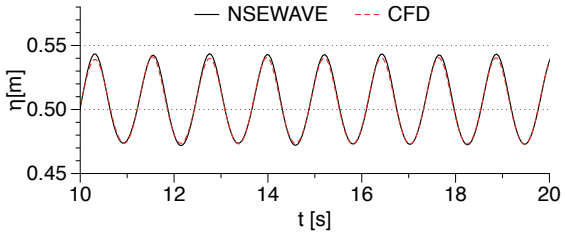

(a) $dx = 0.1$ m at $x = 5$ m

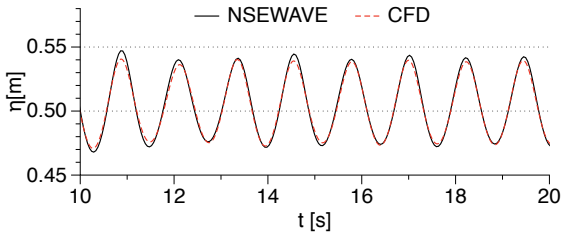

(b) $dx = 0.1$ m at $x = 9$ m

Figure 1: Free surface for incident waves of height $H = 0.07$ m and wavelength $L = 2$ m.

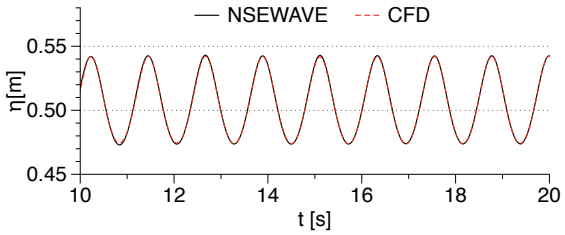

(a) $dx = 0.05$ m at $x = 5$ m

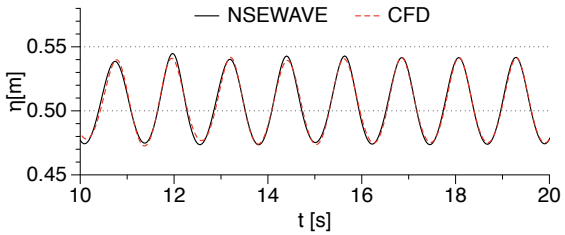

(b) $dx = 0.05$ m at $x = 9$ m

Figure 2: Free surface for incident waves of height $H = 0.07$ m and wavelength $L = 2$ m.

Thus, it is seen that the numerical results from the NSEWAVE approach and the CFD approach provide similar results and the results at $dx = 0.025$ m agree very well with the theoretically expected free surface elevation. The major advantage of using the NSE approach is the time taken to run the simulation. So, the time taken to simulate 50 s of the simulation with the presented wave for the different grid sizes on 128 cores on the high performance computing resource provided at NTNU, *Fram*. Figure 6 presents the change in total time

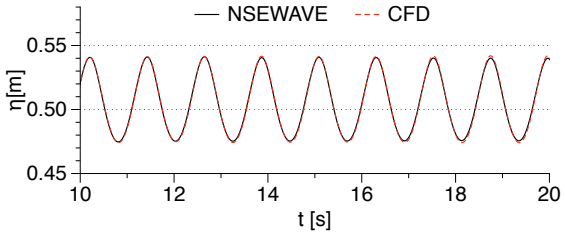

(a) $dx = 0.025$ m at $x = 5$ m

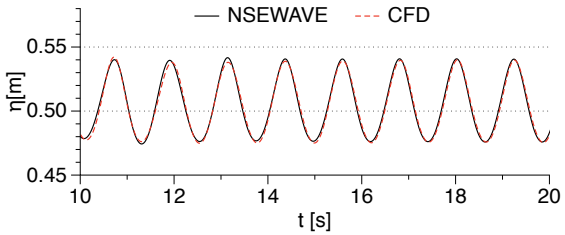

(b) $dx = 0.025$ m at $x = 9$ m

Figure 3: Free surface for incident waves of height $H = 0.07$ m and wavelength $L = 2$ m.

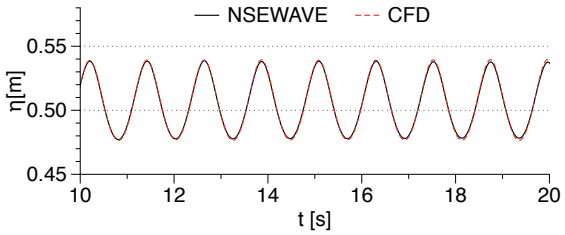

(a) $dx = 0.0125$ m at $x = 5$ m

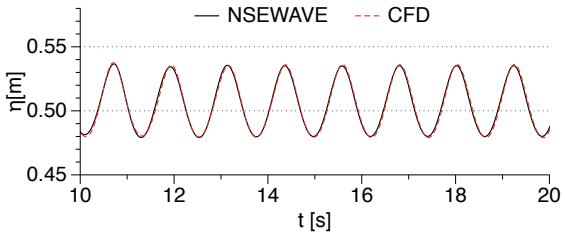

(b) $dx = 0.0125$ m at $x = 9$ m

Figure 4: Free surface for incident waves of height $H = 0.07$ m and wavelength $L = 2$ m.

taken for the simulation for the number of cells in the simulation. It is seen that the NSEWAVE approach completes the simulations much faster. The gain in computational speed using NSEWAVE over CFD is about 4.5.

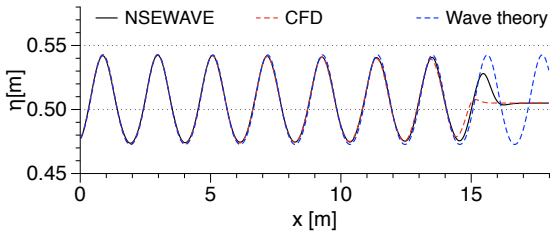

Figure 5: Free surface for incident waves of height $H = 0.07$ m and wavelength $L = 2$ m with NSEWAVE and CFD at $dx = 0.025$m compared with $2nd$-order Stokes wave theory

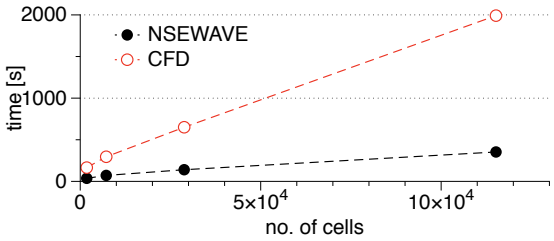

Figure 6: Computing time taken to complete 50 s of the 2D simulation on 128 cores by NSEWAVE and CFD approaches

3.2 Simulation of regular wave interaction with a cylinder

In this section, the interaction of regular waves with a vertical cylinder is investigated using the NSEWAVE approach and the CFD approach in REEF3D. The numerical results are compared to experimental results Chen et al. (2014). The three-dimensional numerical wave tank is 18 m long, 3 m wide and 1 m high with a water depth of $d = 0.505$ m. A cylinder of diameter $D = 0.25$ m is placed at the centre of the tank with its axis at $x = 7.50$ m from the wave generation zone. Regular waves of height $H = 0.07$ m and period $L = 1.22$ s are incident on the cylinder. The simulations are carried out for grid sizes $dx = 0.025$ m, $dx = 0.05$ m and $dx = 0.0125$ m.

The comparison of the computed forces with the experimental data is presented in Figs. 7-9. It is seen from these figures that the agreement of between the results using the NSEWAVE approach is similar to that with the CFD method for the numerically computed wave forces on the cylinder. Further, the free surface elevation in front of the cylinder calculated using the NSEWAVE approach and the CFD approach in REEF3D is compared to the experimental data in Fig. 10 for grid sizes $dx = 0.025$ m and $dx = 0.05$ m. It is seen that the results from NSEWAVE are again very similar to the results obtained using CFD and agree well with the experimental data. The free surface elevation in the numerical wave tank with the horizontal velocity contours at $t = 30$ s is presented in Fig. 11.

The time taken to complete the 3D simulation on 128 cores for the different grid sizes is calculated. The comparison of the time taken by the NSEWAVE approach and the CFD approach is presented in Fig. 12. It is seen that as the number of cells increases, the time taken in the CFD approach increases very quickly compared to the time taken using the NSEWAVE approach. The gain in computational speed by using NSEWAVE for this 3D

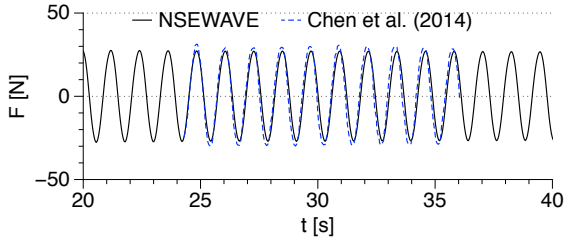

(a) $dx = 0.05$ m using NSEWAVE

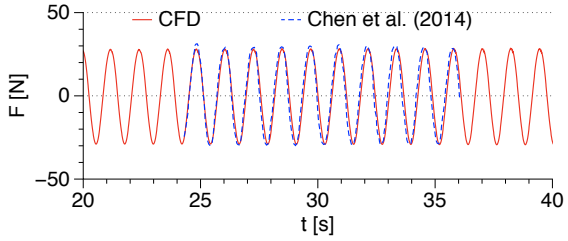

(b) $dx = 0.05$ m using CFD

Figure 7: Wave forces on the cylinder calculated using the NSEWAVE and CFD approach and comparison to experimental data Chen et al. (2014) for incident waves of height $H = 0.07$m and wavelength $L = 2$ m.

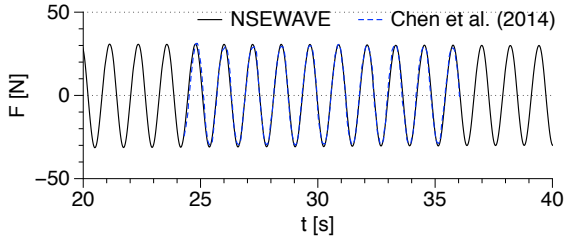

(a) $dx = 0.025$ m using NSEWAVE

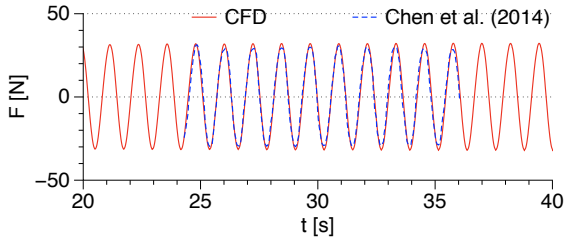

(b) $dx = 0.025$ m using CFD

Figure 8: Wave forces on the cylinder calculated using the NSEWAVE and CFD approach and comparison to experimental dataChen et al. (2014) for incident waves of height $H = 0.07$m and wavelength $L = 2$ m.

simulation compared to the CFD approach is about 7.1. Thus, the use of the NSEWAVE approach can decrease the simulation time taken for several wave simulations. This works to an advantage for the simulation of irregular waves until stationary conditions are reached,

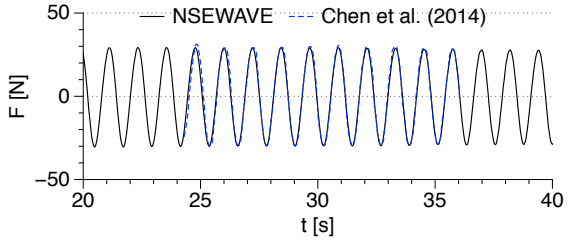

(a) $dx = 0.0125$ m using NSEWAVE

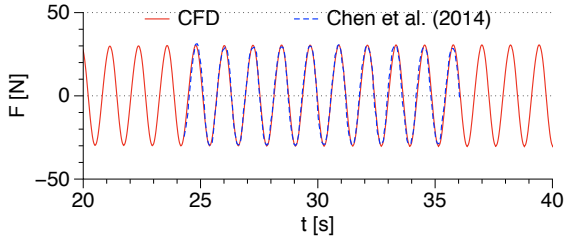

(b) $dx = 0.0125$ m using CFD

Figure 9: Wave forces on the cylinder calculated using the NSEWAVE and CFD approach and comparison to experimental dataChen et al. (2014) for incident waves of height $H = 0.07$m and wavelength $L = 2$ m.

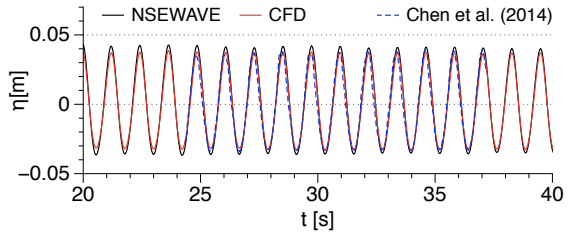

(a) $dx = 0.050$ m

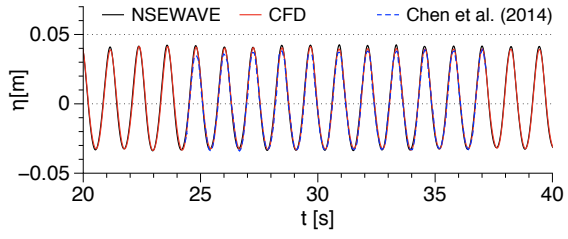

(b) $dx = 0.025$ m

Figure 10: Free surface elevation in front of the cylinder calculated using the NSEWAVE and CFD approach and comparison to experimental dataChen et al. (2014) for incident waves of height $H = 0.07$m and wavelength $L = 2$ m.

identify extreme wave events and simulate large scale problems for numerical wave modelling.

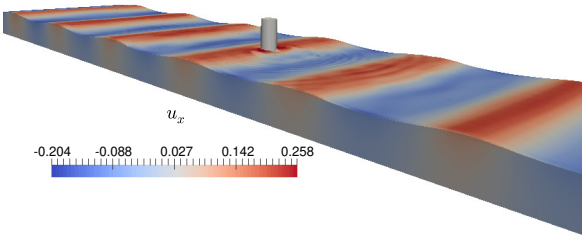

Figure 11: Free surface elevation in the numerical wave tank during wave interaction with a cylinder with horizontal velocity contours

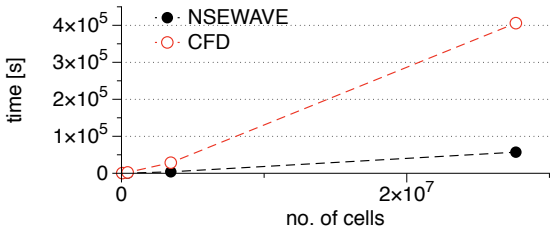

Figure 12: Computing time taken to complete 50 s of the 3D simulation on 128 cores by NSEWAVE and CFD approaches

4 Conclusions

A new approach to calculating the free surface is implemented in the open-source hydrodynamics model REEF3D, utilising interface tracking, a fixed grid and two-phase flow. The free surface is represented using the level set method, while the movement of the free surface is obtained using the continuity principle and the depth integrated horizontal velocity. This provides the advantage that the simulations can be carried out with much coarser grids, larger time steps and thus reducing the computational demand of the simulation. The only compromise is that the level set function is now a single valued function and the model cannot be used to evaluate breaking waves.

The model is used to simulate wave propagation in a numerical wave tank without structures. The numerical results obtained using REEF3D::NSEWAVE are then compared to the results obtained using REEF3D::CFD and the expected free surface elevation using wave theory. It is seen that in the 2D simulation, the NSEWAVE approach provides the same accuracy as the CFD approach while being about 4.5 times faster on computational time. The model is then used to simulate wave interaction with a vertical cylinder. The numerical results for the wave force on the cylinder and the free surface elevation using NSEWAVE is compared with the numerical results obtained using the CFD approach and the experimental data. Again, in the 3D simulation it is seen that the NSEWAVE approach provided similar results to that using the CFD approach for both free surface and wave forces. The computational time used for the 3D simulations using the NSEWAVE approach was about 7.2 times faster than that using the CFD approach.

The novel approach implemented in the open-source hydrodynamics model REEF3D is found to provide similar results to that obtained using the CFD approach, while drastically reducing the computational time. This opens up the opportunity to apply a high resolution phase resolving model to simulate wave engineering problems over large temporal and spatial scales while utilising only a modest amount of computational resources.

Acknowledgements

This research was supported in part with computational resources at NTNU provided by The Norwegian Metacenter for Computational Sciences (NOTUR, http://www.notur.no) under project no. NN2620K.

References

Ai, C., Ding, W. and Jin, S. (2014). A general boundary-fitted 3d non-hydrostatic model for nonlinear focusing wave groups. *Ocean Engineering*, **89**, 134–145.

Ai, C., Jin, S. and Lv, B. (2011). A new fully non-hydrostatic 3d free surface flow model for water wave motions. *International Journal for Numerical Methods in Fluids*, **66**(11), 1354–1370.

Alagan Chella, M., Bihs, H., Myrhaug, D. and Muskulus, M. (2017). Breaking solitary waves and breaking wave forces on a vertically mounted slender cylinder over an impermeable sloping seabed. *Journal of Ocean Engineering and Marine Energy*, **3**(I), 1–19.

Ashby, S.F. and Falgout, R.D. (1996). A parallel mulitgrid preconditioned conjugate gradient algorithm for groundwater flow simulations. *Nuclear Science and Engineering*, **124**(1), 145–159.

Berthelsen, P.A. and Faltinsen, O.M. (2008). A local directional ghost cell approach for incompressible viscous flow problems with irregular boundaries. *Journal of Computational Physics*, **227**, 4354–4397.

Bihs, H., Alagan Chella, M., Kamath, A. and Arntsen, Ø.A. (2017*a*). Numerical investigation of focused waves and their interaction with a vertical cylinder using reef3d. *Journal of Offshore Mechanics and Arctic Engineering*, **139**(4), 041101.

Bihs, H. and Kamath, A. (2017). Simulation of floating bodies with a combined level set/ghost cell immersed boundary representation. *International Journal for Numerical Methods in Fluids*, **83**(12), 905–916.

Bihs, H., Kamath, A., Alagan Chella, M., Aggarwal, A. and Arntsen, Ø.A. (2016*a*). A new level set numerical wave tank with improved density interpolation for complex wave hydrodynamics. *Computers & Fluids*, **140**, 191–208.

Bihs, H., Kamath, A., Alagan Chella, M. and Arntsen, Ø.A. (2016*b*). Breaking-wave interaction with tandem cylinders under different impact scenarios. *Journal of Waterway, Port, Coastal, and Ocean Engineering*.

Bihs, H., Kamath, A., Alagan Chella, M. and Arntsen, Ø.A. (2017*b*). Extreme wave generation, breaking and impact simulations with reef3d. In: *ASME 2017 36th International Conference on Ocean, Offshore and Arctic Engineering, OMAE*.

Chen, L.F., Zang, J., Hillis, A.J., Morgan, G.C.J. and Plummer, A.R. (2014). Numerical investigation of wave–structure interaction using openFOAM. *Ocean Engineering*, **88**, 91—109.

Choi, D.Y., Wu, C.H. and Young, C.C. (2011). An efficient curvilinear non-hydrostatic model for simulating surface water waves. *International Journal for Numerical Methods in Fluids*, **66**(9), 1093–1115.

Chorin, A. (1968). Numerical solution of the Navier-Stokes equations. *Mathematics of Computation*, **22**, 745–762.

Durbin, P.A. (2009). Limiters and wall treatments in applied turbulence modeling. *Fluid Dynamics Research*, **41**, 1–18.

Engsig-Karup, A.P. (2006). *Unstructured nodal DG-FEM solution of high-order boussinesq-type equations*. Ph.D. thesis, Technical University of Denmark, Lyngby.

Falgout, R., Cleary, A., Jones, J., Chow, E., Henson, V., Baldwin, C., Brown, P., Vassilevski, P. and Yang, U. (2010). *HYPRE: High Performance Preconditioners, Users Manual, ver. 2.11*. Center for Applied Scientific Computing, Lawrence Livermore National Laboratory, California, USA.

Harten, A. (1983). High resolution schemes for hyperbolic conservation laws. *Journal of Computational Physics*, **49**, 357–393.

Higuera, P., Lara, L.J. and Losada, I.J. (2013). Realistic wave generation and active wave absorption for Navier-Stokes models application to OpenFOAM. *Coastal Engineering*, **71**, 102–118.

Jacobsen, N.G., Fuhrman, D.R. and Fredsøe, J. (2012). A wave generation toolbox for the open-source CFD library: OpenFOAM. *International Journal for Numerical Methods in Fluids*, **70**(9), 1073–1088.

Jiang, G.S. and Shu, C.W. (1996). Efficient implementation of weighted ENO schemes. *Journal of Computational Physics*, **126**, 202–228.

Kamath, A., Alagan Chella, M., Bihs, H. and Arntsen, Ø.A. (2015*a*). CFD investigations of wave interaction with a pair of large tandem cylinders. *Ocean Engineering*, **108**, 738–748.

Kamath, A., Alagan Chella, M., Bihs, H. and Arntsen, Ø.A. (2015*b*). Evaluating wave forces on groups of three and nine cylinders using a 3D numerical wave tank. *Engineering Applications of Computational Fluid Mechanics*.

Kamath, A., Alagan Chella, M., Bihs, H. and Arntsen, Ø.A. (2016*a*). Breaking wave interaction with a vertical cylinder and the effect of breaker location. *Ocean Engineering*, **128**, 105–115.

Kamath, A., Bihs, H., Alagan Chella, M. and Arntsen, Ø.A. (2016*b*). Upstream-cylinder and downstream-cylinder influence on the hydrodynamics of a four-cylinder group. *Journal of Waterway, Port, Coastal, and Ocean Engineering*. 10.1115/1.404317910.1061/(ASCE)WW.1943-5460.0000339.

Ma, G., Farahani, A.A., Kirby, J.T. and Shi, F. (2016). Modeling wave-structure interactions by an immersed boundary method in a σ-coordinate model. *Ocean Engineering*, **125**, 238–247.

Ma, G., Shi, F. and Kirby, J.T. (2012). Shock-capturing non-hydrostatic model for fully dispersive surface wave processes. *Ocean Modeling*, **43–43**, 22–35.

Naot, D. and Rodi, W. (1982). Calculation of secondary currents in channel flow. *Journal of the Hydraulic Division, ASCE*, **108**(8), 948–968.

Peskin, C.S. (1972). Flow patterns around the heart valves. *Journal of Computational Physics*, **10**, 252–271.

Stelling, G. and Zijlema, M. (2003). An accurate and efficient finite-difference algorithm for non-hydrostatic free-surface fow with application to wave propagation. *International Journal for Numerical Methods in Fluids*, **43**, 1–23.

Stelling, S.G. and Van Kester, J.A.T.M. (1994). On the approximation of horizontal gradients in sigma co-ordinates for bathymetry with steep bottom slopes. *International Journal for Numerical Methods in Fluids*, **18**, 915–935.

Wilcox, D.C. (1994). *Turbulence modeling for CFD*. DCW Industries Inc., La Canada, California.

Young, C.C. and Wu, C.H. (2010). A σ-coordinate non-hydrostatic model with embedded boussinesq-type-like equations for modeling deep-water waves. *International journal for numerical methods in fluids*, **63**(12), 1448–1470.

Zijlema, M. and Stelling, G. (2008). Efficient computation of surf zone waves using the nonlinear shallow water equations with non-hydrostatic pressure. *Coastal Engineering*, **55**(780–790).

Zijlema, M., Stelling, G. and Smit, P. (2005). Further experiences with computing non-hydrostatic free-surface flows involving water waves. *International Journal for Numerical Methods in Fluids*, **48**, 169–197.